Title
Designing a Block Copolymer Membrane for Selective Transport of Lactic Acid from Aqueous Mixtures

Journal
Macromolecules, 58(5)

ISSN
0024-9297

Authors
Jana, Rounak
Gido, Lily A
Halat, David M
et al.

Publication Date
2025-03-11

DOI
10.1021/acs.macromol.4c03089

Designing a Block Copolymer Membrane for Separating Lactic Acid from Aqueous Mixtures

Rounak Jana,[1,2] Lily A. Gido, [1,2] David M. Halat,[2] Carol Sempira,[3] Jeffrey Fedenko,[4] A.P. van Bavel, [5] and Nitash P. Balsara[1,2,]*

[1]Department of Chemical and Biomolecular Engineering, University of California, Berkeley, CA 94720, USA

[2]Materials Sciences Division, Lawrence Berkeley National Laboratory, Berkeley, CA 94720, USA

[3]Shell International Exploration and Production, 3333 Hwy 6 S., Houston, TX 77082, USA

[4]Shell Oil Products US, 150 N Dairy Ashford., Houston, TX 77079, USA

[5]Shell Global Solutions International B.V., Grasweg 31, 1031HW Amsterdam, the Netherlands

Corresponding author's email address: nbalsara@berkeley.edu

Abstract

We report the design and synthesis of a triblock-copolymer-based membrane for enabling selective transport of lactic acid from aqueous solutions. This separation is relevant to the production of polylactic acid, one of the few bio-degradable and bio-based polymers with sufficient mechanical strength for practical applications. The end blocks are positively charged with negatively charged lactate counterions. The middle block is polybutadiene (PBD). Due to microphase separation, the charged blocks form channels for transporting lactic acid. The mechanical integrity of the membrane is controlled by crosslinking the PBD block. Transport of lactic acid and water across the membrane was studied by placing the membrane between two chambers, a feed chamber containing aqueous lactic acid solutions, and a receiving chamber containing pure water. The lactic acid concentration in the receiving chamber was monitored as a function of time using conductivity, HPLC, and NMR. The corresponding flux of water from the receiving chamber to the feed chamber was measured using an NMR-based approach. The lactic acid and water permeabilities through our membrane were $(1.12 \pm 0.05) \times 10^{-8}$ cm^2 s^{-1} and $(8.58 \pm 0.75) \times 10^{-9}$ cm^2 s^{-1}. To our knowledge, there are no reports of lactic acid permeabilities through any membrane in the literature. The separation factor of our membrane, $\alpha_{LA/water}$, 1.305 ± 0.123, is comparable to that of membranes used for selective transport of ethanol, despite the fact that lactic acid is a much larger molecule than ethanol. Selective transport of lactic acid in our membrane is governed mainly by differences in solubility; lactic acid is 18 times more soluble in the membrane than water.

To be used for table of content:

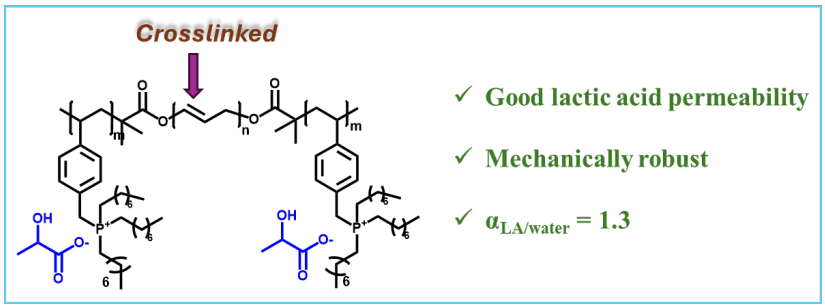

Introduction

There is an increasing demand for lactic acid because poly(lactic acid) (PLA), is one of the few bio-degradable and bio-based polymers with sufficient mechanical strength for practical applications such as packaging.[1–3] Lactic acid is also used in many other industries such as pharmaceuticals, food, cosmetics, and textiles.[4–7] While lactic acid can be produced using standard petroleum-based chemical synthesis, more than 90% of industrially used lactic acid is produced by fermentation of renewable starchy feedstocks such as sugarcane, whey, glycerol, and microalgae.[8–10]

Pure lactic acid is needed because PLA is produced by condensation polymerization, and obtaining high molecular weight polymer samples requires high purity. Traditionally, lactic acid is recovered from the fermentation broth by precipitation.[11] Lactic acid is first precipitated as calcium lactate, and in a second step the precipitate is converted back to lactic acid. The second step requires the use of sulfuric acid which generates toxic chemical waste.[12] A third distillation step is needed to separate the lactic acid from the resulting mixture of lactic acid and water. These three purification steps account for 50% of the total cost of lactic acid.[13] In addition, they are energy-intensive, and most of the current production plants use non-renewable energy.[14] Developing membranes selective toward lactic acid may reduce purification costs. While such membranes could be used to replace distillation by membrane separation, it may be possible to use a membrane to directly obtain pure or reasonably pure lactic acid from the fermentation broth.[15]

There has been relatively little work on the development of membranes that selectively transport lactic acid. Since fermentation results in a dilute lactic acid solution, it is more economical to design a membrane that is selective toward lactic acid (as opposed to water). Processes such as pervaporation cannot be used because the vapor pressure of lactic acid is negligible.[16] We are aware of only two published approaches for membrane-based purification of lactic acid: (1) electrodialysis, and (2) liquid-supported membranes:

(1) Purification of lactic acid using electrodialysis was pioneered by Kentish and coworkers.[17,18] The electrodialysis approach requires both anion exchange and cation exchange membranes. While cation exchange membranes such as Nafion are commercially available and used in industrial processes such as electrochemical production of chlorine gas and hydrogen fuel cells, there are no large-scale industrial processes that rely on anion exchange membranes.

(2) In an important paper, Matsumoto et al. used liquid-supported membranes to purify lactic acid.[19] The membrane was created by incorporating ionic liquids such as trihexyltetradecylphosphonium chloride within a porous polyvinylidene fluoride support. A lactic acid solution with a pH above the pKa of lactic acid served as the feed. The lactate ion enters the membrane and is exchanged for the chloride ion initially present in the membrane. The ionic compound thus formed diffuses to the other side of the membrane which is in contact with a solution maintained at a pH that is below the pKa of lactic acid. The optimized membrane exhibited a lactic acid permeation flux of 7.5×10^{-4} mol m^{-2} h^{-1} μm for a feed concentration of 0.01 mol L^{-1} This approach has many drawbacks. Even though the ionic liquid is extremely hydrophobic, it will dissolve at a finite rate into the surrounding aqueous solutions. The pH of the feed and the purified solutions must be maintained as the lactic acid permeates through the membrane, requiring additional chemicals and purification steps. The most important drawback is that even if these problems are minimized, it is not clear how such a membrane could be implemented. Nevertheless, this work provides a quantitative measure of permeation fluxes that are possible in the context of membranes for lactic acid purification.

Here we report on the synthesis and characterization of an anion exchange membrane that could be used in electrodialysis or other membrane-based separation processes for lactic acid purification. The membrane was based on a triblock copolymer with a crosslinkable polybutadiene (PBD) middle block and poly(4-vinylbenzyl tri n-octyl phosphonium)lactate (PSPL) end blocks. The middle block was crosslinked to obtain the membrane. The membrane comprises microphase-separated PBD and PSPL domains. The PBD domains control the mechanical integrity of the membrane while the PSPL domains provide channels for the selective transport of lactic acid. Both the blocks are chosen to be hydrophobic to minimize water transport.

It is not trivial to design a membrane that selectively transports a bulky molecule like lactic acid relative to a highly mobile molecule like water. Water permeates rapidly even through hydrophobic polymers - this property is exploited in a variety of membrane-based separation processes such as desalination and dehydration of ethanol. The efficacy of membranes is quantified by two transport parameters, permeability of the component of interest and selectivity toward that component. The selectivity of commercial ethanol dehydration membranes, $\alpha_{water/ethanol}$, is often as high as 200. [20] Membranes have also been proposed for

purifying ethanol from ethanol/water mixtures. The selectivity of optimized membranes for this application, $\alpha_{ethanol/water}$, is about 1. [21, 22] This relatively low value of selectivity reflects the unavoidable rapid transport of water through the ethanol selective membranes. The permeation flux through our membrane, when corrected for differences in driving forces, is orders of magnitude higher than that reported in reference 18. The membrane presented in this paper exhibits a lactic acid permeability of $P_{LA} = (1.12 \pm 0.05) \times 10^{-8}$ cm^2/s. The selectivity, $\alpha_{LA/water} = 1.305 \pm 0.123$. Reports of either P_{LA} or $\alpha_{LA/water}$ are lacking in the literature.

Experimental Section

Materials

AIBN was purchased from MilliporeSigma and recrystallized from methanol before use. 4-vinyl benzyl chloride was purchased from MilliporeSigma and passed through a basic alumina column before use. 2-(dodecylthiocarbonothioylthio)-2-methylpropionic acid (RAFT agent), cis-2-butene-1,4-diol, oxalyl chloride, trimethylolpropane tris(3-mercaptopropionate), diphenyl(2,4,6-trimethylbenzoyl)phosphine oxide (TPO), D-lactic acid and tri(n-octylphosphine) were purchased from MilliporeSigma and used as received. The dry solvents (THF and toluene) were also purchased from MilliporeSigma and used as received. Because tri(n-octylphosphine) is air-sensitive, it was stored and used in an argon glovebox.

Synthesis of Polymer and Characterization

The block copolymer from which our membrane was derived was synthesized in three steps shown in **Scheme 1**. A functionalized polybutadiene (PBD) chain was synthesized by ring-opening metathesis polymerization (ROMP) of 1,5 cyclooctadiene in the presence of a 2nd generation Grubb's catalyst. This polymerization was conducted in the presence of a chain transfer agent (molecule 1). Molecule 1 was synthesized by reacting 2-(dodecylthiocarbonothioylthio)-2-methylpropionic acid and cis-2-butene-1,4-diol via an intermediate acid chloride formation (step 1). Molecule 1 is difunctional with reversible addition-fragmentation chain transfer (RAFT) initiators at both ends. The ROMP polymerization results in a difunctional PBD macroinitiator (molecule 2). The molar mass of the macroinitiator was controlled by controlling the ratio of molecule 1 and 1,5 cyclooctadiene. Molecule 1 thus serves two functions – it is both a chain transfer agent and a

RAFT initiator. Our approach for synthesizing molecule 1 is based on reference 22[23], 23[24]. The molar mass of molecule 2 was determined to be 30 kg mol^{-1} using ^{1}H NMR (Figure S2). The GPC trace of molecule 2 is given in Figure S3.

The second monomer (molecule 3), 4-vinylbenzyl(tri n-octylphosphonium)chloride (VBOCl), was synthesized by reacting 4-vinylbenzyl chloride and tri(n-octylphosphine). In the final step, RAFT polymerization VBOCl with PBD macro RAFT initiator results in the growth of two poly 4-vinylbenzyl(tri n-octylphosphonium)chloride blocks at the ends of the macroinitiator. The triblock copolymer (molecule 4) is poly(4-vinylbenzyl(tri n-octylphosphonium)chloride)-*b*-polybutadiene-*b*-poly(4-vinylbenzyl(tri n-octylphosphonium)chloride (PSPL-*b*-PBD-*b*-PSPL). The molar ratio of butadiene monomers to VBOCl was 50:50. The molar ratio PSPL:PBD monomers in the resulting triblock copolymer, determined by ^{1}H and ^{13}C NMR (Figure S5, S6), was 60:40.

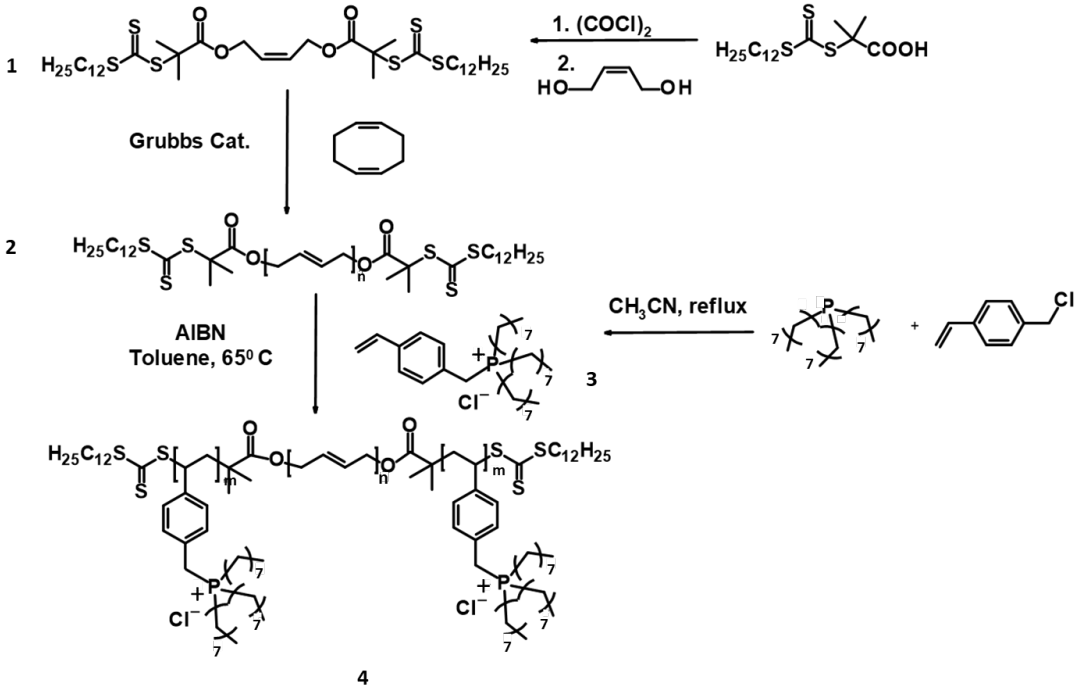

Scheme 1. Synthesis of poly(4-vinylbenzyl(tri n-octylphosphonium)chloride-*b*-polybutadiene-*b*-poly(4-vinylbenzyl(tri n-octyl phosphonium) chloride) (PSPL-b-PBD-b-PSPL) triblock copolymer (4) used to fabricate the membrane. The molar ratio of PSPL to PBD in the final polymer is 60/40.

Membrane Preparation

The membrane preparation steps are given in **Scheme 2**. Molecule 4 was dissolved in chloroform along with a tri-thiol crosslinker, trimethylolpropane tris(3-mercaptopropionate), and a photoinitiator, diphenyl(2,4,6-trimethylbenzoyl)phosphine

oxide (TPO) (molar ratio of crosslinker:initiator was 1:1). The resulting solution was placed on a Teflon disk and subjected to 365 nm UV radiation for 10 mins to form a crosslinked membrane with Cl^- counter anions to give molecule 5. In the final step, this membrane was soaked into a 11.3 mol L^{-1} lactic acid solution for 24 hrs. This results in a crosslinked membrane with lactate counter anions (Figure 1b). The crosslinking and the anion exchange steps were monitored by running FTIR on the film after each stage (Figure S7). The thickness of the membranes made by this approach (l) was 275 ± 30 µm. Based on the chemical structure of the uncrosslinked block copolymer determined by NMR, the ion exchange capacity of the membrane is 1.6 mmol g^{-1}.

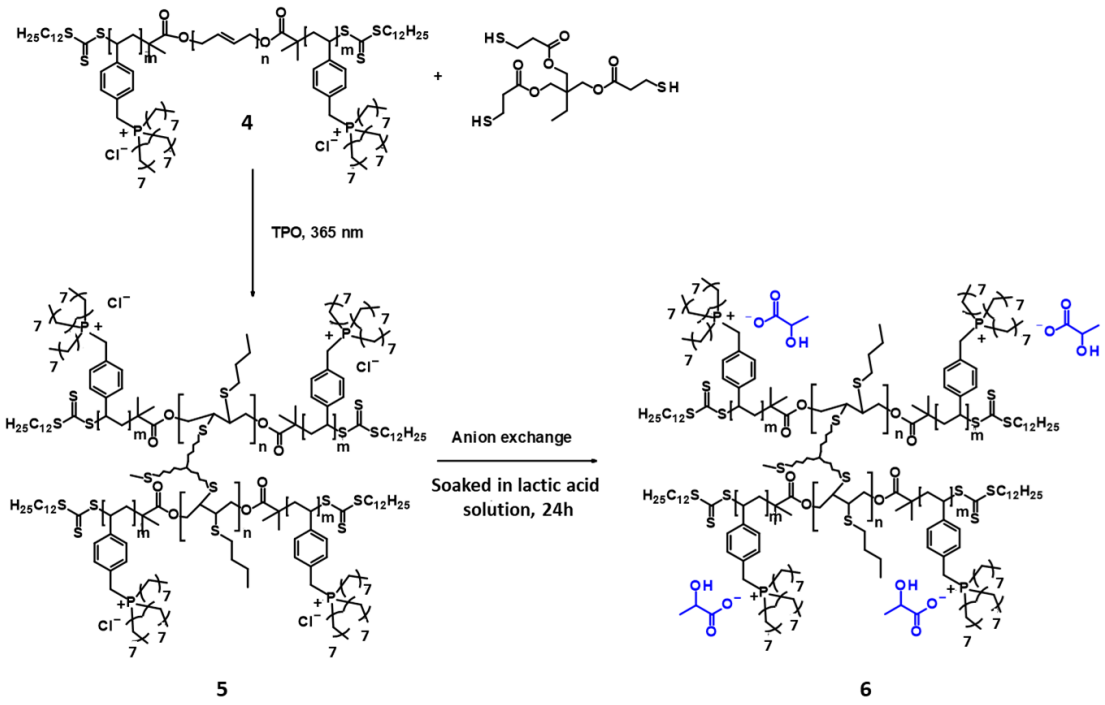

Scheme 2. Preparation of the final crosslinked membranes (6) with lactate counterions. In the first step, the block copolymer (4) was crosslinked using thiol-ene photocuring. In the second step, the crosslinked membrane (5) was soaked in excess lactic acid solution to replace the chloride counterions with lactate counterions.

SAXS Measurements

The morphologies of the crosslinked and uncrosslinked polymers were determined by small-angle X-ray scattering (SAXS) experiments. The samples were inserted in a 1 mm thick annular Viton rubber spacer (McMaster Carr) with an internal diameter of 0.3175 cm and sealed in custom-designed airtight aluminium sample holders with Kapton windows. All the SAXS measurements were conducted at Advanced Light Source beamline 7.3.3 at the Lawrence Berkeley National Lab. Silver behenate was used to determine the beam centre and the sample-to-detector distance. The obtained scattering patterns were azimuthally averaged

using the Nika program for IGOR Pro[25] to produce the one-dimensional scattering profiles; all two-dimensional profiles were azimuthally symmetric. The SAXS intensity, *I*, is reported as a function of the magnitude of the scattering vector, *q*.

$$q = 4\pi \sin(\theta/2)/\lambda\,, \quad (1)$$

where, θ is the scattering angle and λ is the wavelength of the X-ray beam (0.12398 nm).

Transport Experiments

The separation of lactic acid/water mixtures was studied in a "side-bi-side" cell purchased from PermeGear, Inc (Figure 1a). The cell comprises two chambers, each with a volume of 4 ml and was equipped with a stir bar. The ports above the two chambers were sealed with a Teflon cap to prevent water evaporation and contact with moisture in the air. This is especially important for the experiments involving D_2O. The membrane was held in place between the two chambers by screws. The temperature of the cell was kept constant at 24 ± 1 °C by circulating water. Chamber 1 (Figure 1a) was filled with a lactic acid/water solution of a known concentration and chamber 2 was filled with pure water. The concentrations used in chamber 1 were 0.66, 1.15, and 3.08 mol L^{-1}. Milli q water with a conductivity of 3 μS cm^{-1} at 24 ± 1 °C was used in both cells.

The composition of the solutions in the two chambers changes with time due to permeation through the membrane. These changes were monitored using three approaches. Appropriate amounts of the solutions were removed from the chambers for analysis. The primary approach was conductivity, measured using a Mettler Toledo InLab-751 conductivity probe with platinum blocking electrodes at 24 ± 1 °C. The conductivity probe was calibrated using a 1413 μS cm^{-1} potassium chloride conductivity standard to determine the cell constant before each measurement. In some cases, the lactic acid concentration was also determined using HPLC and NMR. The solutions in both chambers were stirred throughout the experiment.

(1) Conductivity: The conductivities of the solutions in both chambers were measured by pipetting 1 ml sample solution from the cells at selected times through the ports. After the conductivity was measured, the solutions were put back into their respective cells. The time required for each conductivity measurement was about 10 min. Typical transport experiments were run for 72 h. Care was taken to ensure that the volumes of solutions in the two chambers were not affected by our procedure. Known concentrations of lactic acid/water mixtures were used to create a calibration plot of concentration vs conductivity

(Figure S8). The transport experiments described here were repeated using three different membranes. The standard deviation of these measurements was taken as the error bar.

(2) HPLC: The concentrations at both chambers were measured by HPLC by pipetting out sample solutions at different time intervals (24, 48, and 72 h) from the cell. In this case, the transport experiments were restarted with fresh solutions after samples were removed for HPLC. The chamber 2 solutions were examined directly by HPLC. Chamber 1 solutions were diluted to ensure that the concentration examined was within the range of the HPLC instrument (0.01 mol L^{-1} to 0.22 mol L^{-1} for lactic acid). Samples were prepared by passaging through a 0.22 µm filter and analysed on a ThermoScientific Vanquish with a RefractoMax 520 detector. A BioRad Aminex HPX-87H column and H column guard were maintained at 65°C and 0.45 mL/min mobile phase flow rate of 0.005 M H_2SO_4. The refractive index detector was operated at 50°C and post-column cooler was operated at 40°C.

^{1}H NMR: The concentrations of both chambers were also measured by ^{1}H NMR. ^{1}H NMR spectra were recorded on a Bruker Avance I spectrometer with a 5 mm BBO probe (^{1}H, 400 MHz) referenced to the residual HDO peak at 4.79 ppm. Separate experiments were carried out to determine lactic acid flux and water flux. These experiments were only conducted for the 3.08 mol L^{-1} lactic acid solution.

For determining lactic acid flux in chamber 2, chamber 1 was filled with a 3.08 mol L^{-1} lactic acid /H_2O solution, and chamber 2 was filled with D_2O. 0.5 ml of the solution was taken out from chamber 2 and placed in an NMR tube along with 10 µL of an internal standard solution (0.0028 mol L^{-1} solution of Me_3Si-C_2D_4-COOH in 0.5 mL D_2O solution) at different time intervals (4, 24, 48, and 72 h). The lactic acid concentrations in chamber 2 were determined using the following equation,

$$c_{LA}(t) = \frac{9I_{1.39}}{3I_{0.0}} \times 0.0028 \text{ mol L}^{-1}, \quad (2)$$

where $I_{1.39}$ is the intensity of the methyl peak of lactic acid at 1.39 ppm and $I_{0.0}$ is the intensity of the three methyl peaks at 0.0 ppm of Me_3Si-C_2D_4-COOH. The number of scans was kept constant at 32. A 2 s delay was applied between pulses without employing receiver gain. The transport experiments were restarted with fresh solutions after samples were removed for NMR.

For determining the water flux from chamber 2 to chamber 1, chamber 1 was filled with a 3.08 mol L^{-1} lactic acid /D_2O solution, and chamber 2 was filled with H_2O. The concentration of chamber 1 as a function of time was determined using the same NMR protocols described above. Alongside each transport experiment, a 0.5 ml 3.08 mol L^{-1} lactic

acid in D_2O containing the internal standard was prepared and examined by NMR at the same time. This spectrum was used to determine the background HDO intensity due to H/D exchange. The water concentrations in chamber 1 were determined using the following equation,

$$c_w(t) = \frac{9\left(I_{4.79} - I_{4.79}(b)\right)}{2I_{0.0}} \times 0.0028 \text{ mol L}^{-1}, \quad (3)$$

where $I_{4.79}$ is the intensity of HDO at 4.79 ppm, $I_{4.79}(b)$ is the background HDO intensity, and $I_{0.0}$ was defined earlier.

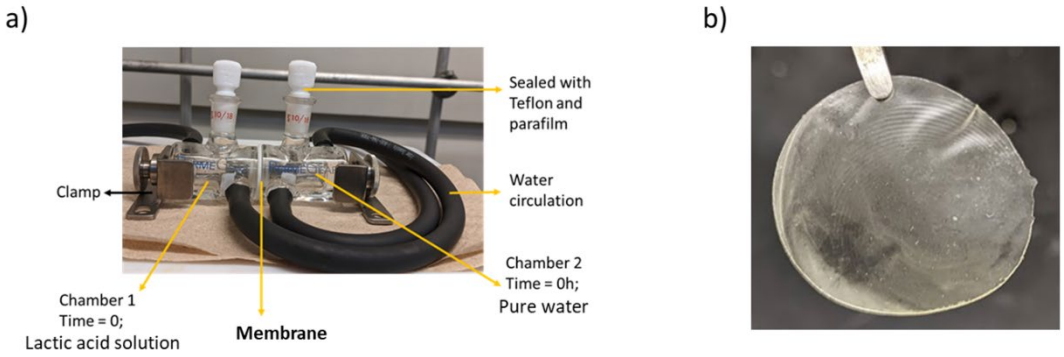

Figure 1. Image of the cell used to measure the flux of lactic acid and water through the membrane (a), and the final membrane (b). The cell design was taken from the work of Beckingham et al.[27] The thickness of the membranes was 275 ± 30 µm. The membranes were self-standing and mechanically stable during the experiments that lasted over a month.

Permeability and selectivity calculation

The permeability of lactic acid through the membrane, P_{LA}, in the apparatus described in Figure 1a, is given by,[26,27,28]

$$P_{LA} = \ln\left(1 - \frac{2c_{LA}(t)}{c_{LA0}}\right)\left(\frac{-lv}{2At}\right), \quad (4)$$

where $c_{LA}(t)$ is the concentration of lactic acid in chamber 2 at time t, c_{LA0} is the concentration of lactic acid in chamber 1 at time $t = 0$, l is the membrane thickness (275 µm), v is the volume of each chamber (4 mL), and A is the area of the membrane separating the two solutions (0.518 cm^2). Equation 4 assumes that changes in the concentration of chamber 1 are negligible.

Water permeability, P_{water} is given by,

$$P_{water} = \ln\left(1 - \frac{2c_w(t)}{c_{wo}}\right)\left(\frac{-lv}{2At}\right), \quad (5)$$

where $c_w(t)$ is the concentration of water in chamber 1 at time t, c_{w0} is the concentration of water in chamber 2 at time $t = 0$.

The lactic acid separation factor, $\alpha_{LA/water}$, is given by,[21]

$$\alpha_{LA/water} = P_{LA}/P_{water}. \quad (6)$$

Uptake measurements

The uptake measurements were carried out on the membrane using the following lactic acid solutions, 0.66, 1.15, 1.74, 2.45, and 3.08 mol L^{-1}. The concentrations of the external solutions in units of g cm^{-3}, $m_{LA,external}$, and $m_{water,external}$, were determined using the known densities of lactic acid and water, 1.2 and 1.0 g cm^{-3}, ignoring volume change of mixing. Pieces of the membrane, weighing between 0.1 and 0.2 g, were used in these experiments. First, the weight of the dry membrane (w_{dry}) was measured. Then, the membrane was soaked in the lactic acid solution of interest for 24 hours. After that, it was taken out from the solution, and the residual solution on the surface was carefully wiped using a Kim wipe, and the weight of the wet membrane (w_{wet}) was measured. The total uptake of water and lactic acid was calculated by taking the difference in weight between the wet and the dry membrane. After that, the wet membrane was soaked in 10 ml (excess) milli q water for 48 h to allow the absorbed lactic acid to leach into the water. The concentration of lactic acid in the water ($c_{LA,uptake}$) was determined by measuring the conductivity of this water solution, and converting the conductivity to concentration using the lactic acid concentration versus conductivity calibration curve used to interpret the transport measurements (Figure S8). The density of the membrane (ρ_m) was determined by dividing the mass of the membrane by its volume, $\rho_m = 0.714 \pm 0.15$ g cm^{-3}. The uptake in g of lactic acid and water per cm^3 of membrane, $m_{LA,}$ and m_{water}, was then calculated using the following equations,

$$m_{LA} = \frac{c_{LA,uptake} \times 10 \times 90.08}{(\frac{W_{dry}}{\rho_m}) \times 1000}, \quad (7)$$

and

$$m_{water} = \left(\frac{W_{wet} - (m_{LA} \times (\frac{W_{dry}}{\rho_m}))}{(\frac{W_{dry}}{\rho_m})} \right). \quad (8)$$

Uptake results are presented on plots of m_i versus $m_{i,external}$ (i = LA or water). (Figure 8)

Result and discussion

Small-angle X-ray scattering (SAXS) profiles of the uncrosslinked PSPL-*b*-PBD-*b*-PSPL block copolymer and the crosslinked membrane are shown in Figure 2. Both profiles exhibit shoulders at $q \approx 0.2$ nm^{-1}. This indicates the presence of the weakly ordered PSPL–rich, and PBD–rich domains. The PSLA-rich domains provide avenues for selected lactic acid transport while the crosslinked PBD-rich provide the membrane with mechanical integrity. The estimated thicknesses of the PSPL-rich and the PBD-rich domains are 18 and 12 nm, based on the SAXS data and the block copolymer composition. The domain structure present in the uncrosslinked block copolymer is preserved after crosslinking.

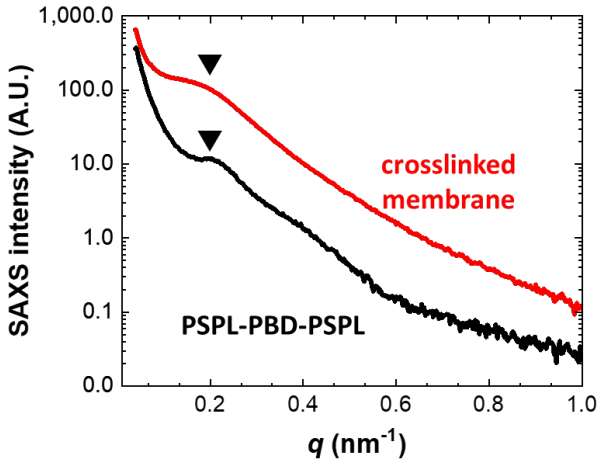

Figure 2. SAXS intensity of (PSPL-PBD-PSPL) (4) and the final crosslinked membrane (6) plotted as a function of the magnitude of the scattering vector *q*. The triangles indicate the locations of broad peaks superposed on a sloping background. The domain spacing corresponding to the center-to-center distance between the adjacent PSPL domains is approximately 30 nm in both cases.

The separation experiments were carried out in the separation cell discussed in the experimental section and shown in Figure 1a. The lactic acid solutions of interest were placed in chamber 1 and pure water was placed in chamber 2. The difference in lactic acid chemical potential drives the diffusion of lactic acid from chamber 1 to chamber 2 through the membrane. The difference in water chemical potential drives the diffusion of water from chamber 2 to chamber 1. The change in lactic acid concentration in both chambers was monitored as described in the experimental section.

In Figure 3, we show the time dependence of lactic acid concentration in chambers 1 and 2 determined by conductivity when the initial lactic acid concentration in chamber 1 (c_{LA0}) was 3.08 mol L^{-1}. The lactic acid concentration in chamber 2, c_{LA}, increases monotonically due to diffusion of lactic acid into chamber 2. In contrast, changes in the lactic acid concentration in chamber 1 are not detectable. To a good approximation, the lactic acid concentration in chamber 1 remains constant at a value close to c_{LA0}. The measured concentration in chamber 1 is not identical to c_{LA0} due to experimental error in our calibration-based approach. In other words, the diffusion of water from chamber 2 to chamber 1 cannot be detected by conductivity. This is due to the large concentration of water already present at t = 0 in chamber 1. The conductivity experiments are mainly geared toward determining the lactic acid flux through the membrane. Similar results were obtained in all our experiments; Figure S9 where the initial chamber 1 concentration was at c_{LA0} = 1.15 mol L^{-1}.

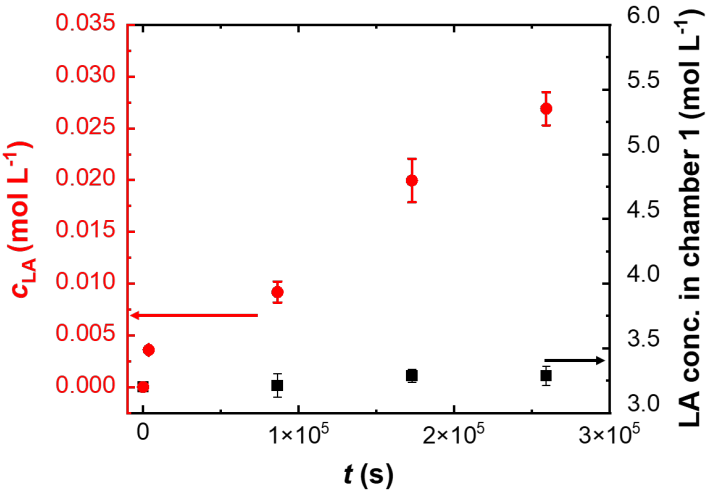

Figure 3. Typical data obtained from the transport experiments using conductivity to determine the lactic acid concentrations in chambers 1 and 2. The initial lactic acid concentration at chamber 1, c_{LA0} = 3.08 mol L^{-1}. Lactic acid concentration in chamber 2, c_{LA}, is plotted against time, t, using the left y-axis. Lactic acid concentration in chamber 1 is plotted against time, t, using the right y-axis. The chamber 1 lactic acid concentration is more-or-less independent of time, and it is approximately equal to c_{LA0}.

In Figure 4, we plot the lactic acid concentration in chamber 2 (c_{LA}) determined by conductivity, HPLC, and NMR as a function of time when the initial LA concentration in chamber 1 (c_{LA0}) is 3.08 mol L^{-1}. The agreement between the three methods is reasonable, despite the significant difference in experimental details and methodologies. We focused on c_{LA} measurements using conductivity because it was the most convenient approach and did not involve restarting the experiments after measuring lactic acid concentration. The data in Figure 3 demonstrates the validity of the conductivity-based approach. The importance of the NMR measurements will be clarified shortly.

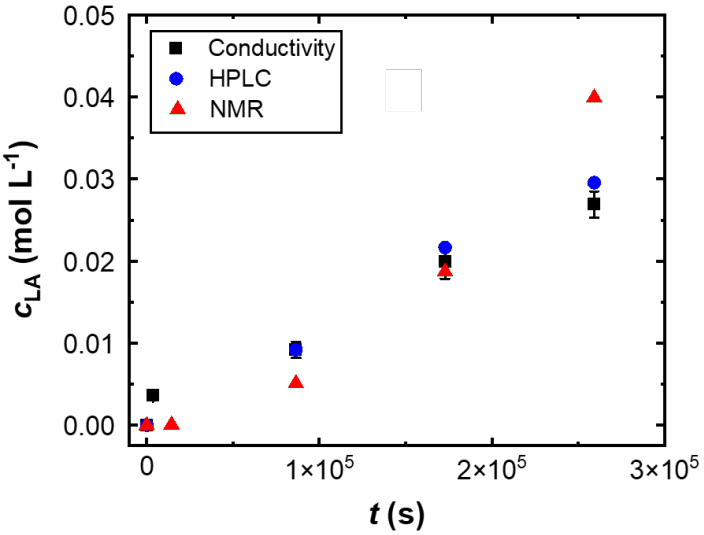

Figure 4. Typical data obtained from the transport experiments using conductivity to determine the lactic acid concentrations. The initial lactic acid concentration at chamber 1, c_{LA0} = 3.08 mol L^{-1}. Lactic acid concentration in chamber 2, c_{LA}, is plotted against time, t, using conductivity (black square), HPLC (blue circles), and ^{1}H NMR measurements (red triangles). The results obtained from the three techniques agree reasonably well.

In Figure 5a, we plot c_{LA} determined by conductivity as a function of time for all three values of c_{LA0} (0.66, 1.15, and 3.08 mol L^{-1}). Increasing c_{LA0} results in an increase in the rate at which lactic acid diffuses into chamber 2. The curves in Figure 5a represent a quadratic fit through the origin corresponding to each dataset. In Figure 5b, we plot c_{LA} determined by HPLC as a function of time for all three values of c_{LA0}. For convenience, the quadratic fits through the data in Figure 5a are also shown in this plot. The agreement between conductivity and HPLC experiments is reasonable. The agreement at c_{LA0} = 3.08 mol L^{-1} is within experimental error. At lower values of c_{LA0}, the values of c_{LA} determined by HPLC lie below those determined by conductivity.

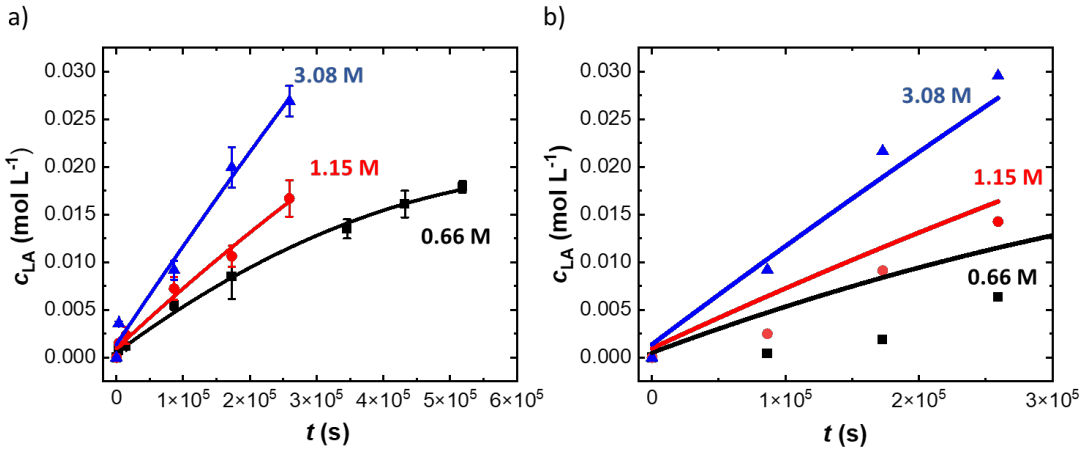

Figure 5. The time dependence of lactic acid concentration at chamber 2, c_{LA}, for different values of initial lactic acid concentration in chamber 1, c_{LA0} = 0.66, 1.15, and 3.08 mol L^{-1}. (a) The datapoints were obtained using conductivity. The curves represent a quadratic fit through the origin corresponding to each dataset. (b) The datapoints were obtained using HPLC. The curves represent data based on conductivity, taken from Figure 5a.

In Figure 6, we combine the time dependence of c_{LA} measured using conductivity, HPLC, and NMR for all values of c_{LA0} by plotting $\ln(1-(2c_{LA}(t)/ c_{LA0})$ versus time. To a good approximation, all the data collapse onto a single line, as predicted by the theory of Yasuda et al. [28] We used the slope of this line in conjunction with equation 4 to determine the permeability of lactic acid through the membrane, P_{LA}. This gives $P_{LA} = (1.12 \pm 0.05) \times 10^{-8}$ cm^2 s^{-1}.. For c_{LA0} = 1.15 mol L^{-1}, the flux of lactic acid through our membrane is 8.51×10^2 mol m^{-2} h^{-1}μm, almost 6 orders of magnitude higher than that reported in reference 18. We estimate that our permeation flux, normalized for concentration differences is about 4 orders of magnitude larger than that reported in reference 18. This is because permeation flux is approximately proportional to difference in concentrations and the concentration of lactic acid used in reference 18 was about 2 orders of magnitude lower than that used in our study.

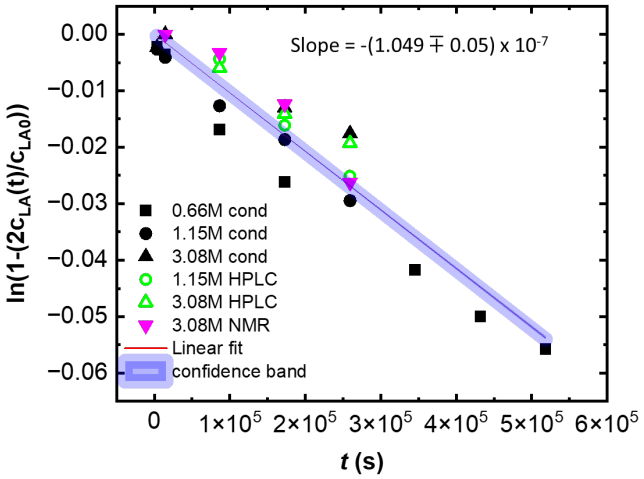

Figure 6. Analysis of lactic acid transport experiments. c_{LA} is the time-dependent lactic acid concentration in chamber 2. Data obtained using different values of initial lactic acid concentration in chamber 1, c_{LA0} = 0.66, 1.15, and 3.08 mol L^{-1}, and different techniques (conductivity, HPLC, and NMR) are shown. All the data, when plotted as $\ln(1-(2c_{LA}(t)/ c_{LA0})$ versus time, collapse on a line, consistent with the theory of Yasuda et al. [28] The slope of the least-squares linear fit through the data gives the permeability of lactic acid through the membrane, P_{LA} = (1.12 ± 0.05) $\times 10^{-8}$ cm^2 s^{-1}.

In Figure 7a, we show the time dependence of H_2O concentration in chamber 1 determined by NMR when the initial lactic acid concentration in chamber 1 (c_{LA0}) was 3.08 mol L^{-1}. Recall that the initial solution in chamber 1 was made using D_2O. We use equation 3

to calculate $c_w(t)$. The curve in Figure 7a represents a quadratic fit through the origin. The flux of H_2O from chamber 2 to chamber 1, which could not be discerned from conductivity and HPLC experiments, is clearly seen in the NMR experiments. In Figure 7b we plot $\ln(1-(2c_w(t)/c_{w0})$ versus time. c_{w0} = 55.6 mol L^{-1} corresponding to the presence of pure water in chamber 2 at $t = 0$. To a good approximation, all the data collapse onto a single line. We used the slope of this line in conjunction with equation 5 to determine the permeability of water through the membrane, P_{water}. This gives $P_{water} = (8.58 \pm 0.75) \times 10^{-9}$ cm^2 s^{-1}. The water flux into chamber 1 is about 0.02 mL in 72 hours. This is very small compared to the volume of chamber 1 (4 mL). Attempts to measure volume changes of chamber 1 were, not surprisingly, unsuccessful.

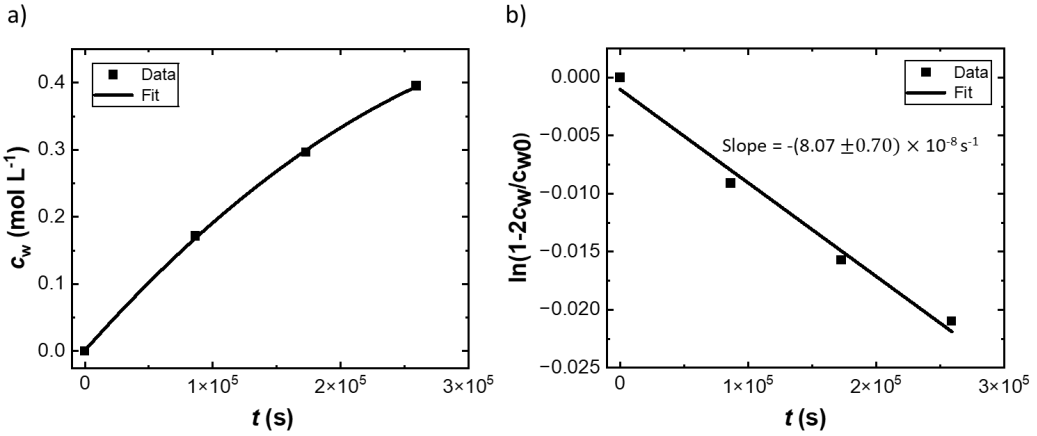

Figure 7. (a) Data obtained from the transport experiments using NMR to determine the the time-dependence of water concentrations, c_w, in chamber 1. The initial lactic acid concentration in chamber 1, c_{LA0} = 3.08 mol L^{-1}. This solution was made using D_2O. The curve represents a quadratic fit through the origin. (b) Plot of $\ln(1-(2c_w(t)/c_{w0})$ versus time. c_{w0} = 0.0556 mol L^{-1} corresponding to the presence of pure water in chamber 2 at $t = 0$. The slope of the least-squares linear fit through the data was used to calculate the water permeability, $P_{water} = (8.58 \pm 0.75) \times 10^{-9}$ cm^2 s^{-1}.

The separation factor of our membrane, $\alpha_{LA/water}$, is 1.305 ± 0.123 (see equation 6). To our knowledge this is the only reported value of separation factor for aqueous lactic acid mixtures. It is comparable to the separation factor of optimized membranes for aqueous ethanol mixtures. [21 22] This is noteworthy because lactic acid is a much larger molecule than ethanol.

The transport of a species through a membrane is often explained by the solution diffusion model. [29,30] According to this model, this transport takes place by dissolution of the solute from the high concentration chamber into the membrane, followed by diffusion of the

solute through the membrane, and finally, dissolution of the solute from the membrane into the low concentration chamber. In this model, the permeability of species *i* is expressed as,

$$P_i = K_i D_i, \quad (9)$$

where K_i is the solubility coefficient of species *i* in the membrane, which is given as, [28]

$$K_i = \left(\frac{m_i}{m_{i,\text{external}}}\right), \quad (10)$$

and D_i the diffusivity of *i* through the membrane. While solubility depends on the thermodynamic interaction between the membrane and species *i*, diffusivity depends on the size of the diffusing species and the environment presented by the membrane.

The results of lactic acid and water uptake experiments are shown in Figure 8. In Figure 8a m_{LA} is plotted against $m_{\text{LA,external}}$. In Figure 8b, m_{water} is plotted against $m_{\text{water,external}}$. The lines in both plots are linear fits through the origin that give $K_{LA} = 0.53 \pm 0.04$ and $K_{water} = 0.029 \pm 0.001$.The diffusion coefficients obtained using equation 9 with measured values of P_i and K_i are $D_{\text{LA}} = (2.10 \pm 0.17) \times 10^{-8}$ cm^2 s^{-1} and $D_{\text{water}} = (2.89 \pm 0.54) \times 10^{-7}$ cm^2 s^{-1}. The value of D_{water} is low, relative to published values of diffusion coefficients of water in hydrophobic polymers. For example, the diffusion coefficient of water in a commercial rubber, ethylene propylene diene monomer (EPDM) is about 10^{-6} cm^2 s^{-1}. [31] The fact that D_{LA} is about an order of magnitude smaller than D_{water} is not surprising, given the large differences in molar mass. This analysis indicates that the selective transport of lactic acid in our membrane is dominated by solubility effects.

Our determination of the solubility parameters, K_{LA} and K_{water}, and the diffusivities, D_{LA} and D_{water} gives us important insight into the underpinnings of the selective transport of lactic acid. Since we designed our membrane to be hydrophobic but with lactic-acid-compatible components, lactic acid dissolves 18 times higher than water inside our membrane. However, water has a much smaller molecular size than lactic acid. As a result, the small amount of dissolved water diffuses through the membrane 14 times faster than the large amount of dissolved lactic acid, making the overall lactic acid permeability, P_{LA} only 1.3 times higher than the water permeability, P_{water} for our membrane.

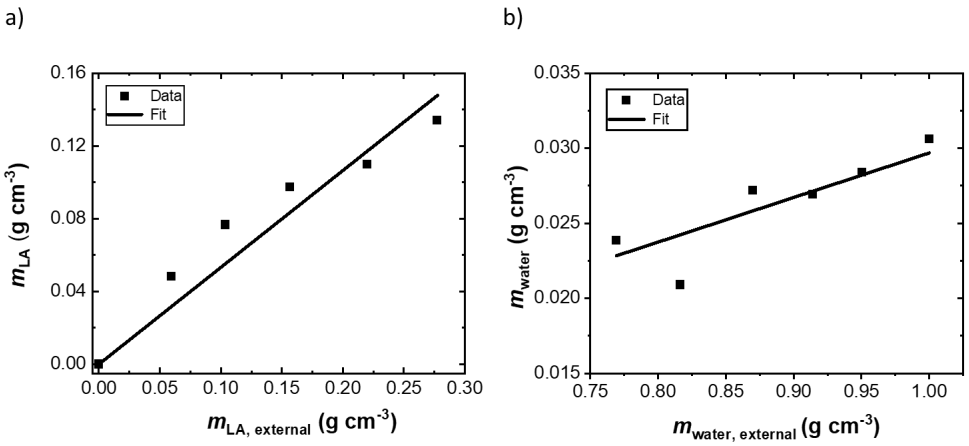

Figure 8. Data related to solubility of lactic acid and water in the membrane obtained by equilibrating the membrane in different external lactic acid solutions. (a) The mass-based concentration of lactic acid in the membrane, $m_{LA,}$ is plotted as a function of lactic acid concentration in the external solution, $m_{LA,external}$. (b) The water concentration in the membrane, m_{water}, is plotted as a function of water concentration in the external solution, $m_{water,external}$. The slopes of the least-squares fit through the data lines give solubility coefficients, $K_{LA} = 0.53 \pm 0.04$ and $K_{water} = 0.029 \pm 0.001$.

Conclusions

We report the design and synthesis of a PSPL-PBD-PSPL triblock-copolymer-based membrane for enabling selective transport of lactic acid from aqueous solutions. Due to microphase separation, the PSPL blocks form channels for transporting lactic acid in a matrix of mechanically robust crosslinked PBD. Our approach allows for independent control over transport and mechanical properties of the membrane. The PSPL blocks are positively charged with negatively charged lactate counterions. Our design assumed that the presence of lactate counterions would facilitate the transport of lactic acid. This approach has general implications because the lactate counterions can be exchanged for any other anion, thereby, facilitating the transport of other charged species, cations or anions.

The membrane was placed between two chambers, a feed chamber containing aqueous lactic acid solutions, and a receiving chamber containing pure water. The lactic acid concentration in the receiving chamber was monitored as a function of time using conductivity, HPLC, and NMR. Results from all three techniques are in reasonable agreement and consistent with the model proposed by Yasuda et al.,[28] normalized for differences in concentration. The

lactic acid permeability, determined from our measurements, was $(1.12 \pm 0.05) \times 10^{-8}$ cm^2 s^{-1}. The corresponding flux of water from the receiving chamber to the feed chamber was measured using an NMR-based approach. The water permeability, determined from our measurements, was $(8.58 \pm 0.75) \times 10^{-9}$ cm^2 s^{-1}. The separation factor of our membrane, $\alpha_{LA/water}$, is 1.305 ± 0.123. To our knowledge, there are no previous reports of either lactic acid permeability or separation factor in the literature. The transport of a given species through a membrane depends on both solubility and diffusivity. Uptake measurements were used to distinguish between these two parameters. Selective transport of lactic acid in PSLA-PBD-PSLA membrane is governed mainly by differences in solubility; lactic acid is 18 times more soluble than water.

In conclusion, we have successfully designed an ionic membrane to selectively transport lactic acid. Our hypothesis was that a polymer with lactate counterions would facilitate the selective transport of our target molecule. Our membrane is also technically an anion exchange membrane. Much of the work in anion-exchange-membrane literature is geared toward enabling hydrogen fuel cells with hydroxide working ions.[32] The main scientific challenge in the fuel cell membrane, which contains hydroxide counterions, is chemical degradation of the polymer backbone and side chains in the presence of a base. Our work shows the importance of an entirely different class of charged membranes with counter anions that are free of the degradation challenge. The membrane we have designed may be used as the anion exchange membrane in electrodialysis setups used for lactic acid purification.[17,18] Such technologies are expected to become increasingly important as the fraction of electrical energy obtained from renewable sources increases.

Acknowledgement

This work was supported by the Energy Biosciences Institute funded by Shell. We thank John Coates and Chris Rao for helpful discussions and guidance. We also thank Benny Freeman for his valuable suggestions on transport experiments and Ms. Shreya Makkar for helping us with error analysis. This research used resources of the Advanced Light Source, which is a DOE Office of Science User Facility under contract no. DE-AC02-05CH11231. We acknowledge Advanced Light Source beamline 7.3.3 at the Lawrence Berkeley National Lab for SAXS and Eric Schaible (beamline scientist) for helping us set up the experiment in the beamline.

References:

(1) Komesu, A.; de Oliveira, J. A. R.; da Silva Martins, L. H.; Maciel, M. R. W.; Filho, R. M. Lactic Acid Production to Purification: A Review. *BioResources* **2017**, *12* (2), 4364–4383. https://doi.org/10.15376/BIORES.12.2.KOMESU.

(2) Abdel-Rahman, M. A.; Tashiro, Y.; Sonomoto, K. Recent Advances in Lactic Acid Production by Microbial Fermentation Processes. *Biotechnol. Adv.* **2013**, *31* (6), 877–902. https://doi.org/10.1016/j.biotechadv.2013.04.002.

(3) Okano, K.; Tanaka, T.; Ogino, C.; Fukuda, H.; Kondo, A. Biotechnological Production of Enantiomeric Pure Lactic Acid from Renewable Resources: Recent Achievements, Perspectives, and Limits. *Appl. Microbiol. Biotechnol.* **2010**, *85* (3), 413–423. https://doi.org/10.1007/s00253-009-2280-5.

(4) Lan, K.; Xu, S.; Li, J.; Hu, C. Recovery of Lactic Acid from Corn Stover Hemicellulose-Derived Liquor. *ACS Omega* **2019**, *4* (6), 10571–10579. https://doi.org/10.1021/acsomega.9b00794.

(5) Juturu, V.; Wu, J. C. Microbial Production of Lactic Acid: The Latest Development. *Crit. Rev. Biotechnol.* **2016**, *36* (6), 967–977. https://doi.org/10.3109/07388551.2015.1066305.

(6) Rodrigues, C.; Vandenberghe, L. P. S.; Woiciechowski, A. L.; de Oliveira, J.; Letti, L. A. J.; Soccol, C. R. Production and Application of Lactic Acid. *Curr. Dev. Biotechnol. Bioeng. Prod. Isol. Purif. Ind. Prod.* **2016**, 543–556. https://doi.org/10.1016/B978-0-444-63662-1.00024-5.

(7) Tashiro, Y.; Kaneko, W.; Sun, Y.; Shibata, K.; Inokuma, K.; Zendo, T.; Sonomoto, K. Continuous D-Lactic Acid Production by a Novelthermotolerant Lactobacillus Delbrueckii Subsp. Lactis QU 41. *Appl. Microbiol. Biotechnol.* **2011**, *89* (6), 1741–1750. https://doi.org/10.1007/s00253-010-3011-7.

(8) Abdel-Rahman, M. A.; Tashiro, Y.; Sonomoto, K. Lactic Acid Production from Lignocellulose-Derived Sugars Using Lactic Acid Bacteria: Overview and Limits. *J. Biotechnol.* **2011**, *156* (4), 286–301. https://doi.org/10.1016/j.jbiotec.2011.06.017.

(9) Liu, B.; Yang, M.; Qi, B.; Chen, X.; Su, Z.; Wan, Y. Optimizing L-(+)-Lactic Acid

Production by Thermophile Lactobacillus Plantarum As.1.3 Using Alternative Nitrogen Sources with Response Surface Method. *Biochem. Eng. J.* **2010**, *52* (2–3), 212–219. https://doi.org/10.1016/j.bej.2010.08.013.

(10) Castillo Martinez, F. A.; Balciunas, E. M.; Salgado, J. M.; Domínguez González, J. M.; Converti, A.; Oliveira, R. P. de S. Lactic Acid Properties, Applications and Production: A Review. *Trends Food Sci. Technol.* **2013**, *30* (1), 70–83. https://doi.org/10.1016/j.tifs.2012.11.007.

(11) Wasewar, K. L.; Yawalkar, A. A.; Moulijn, J. A.; Pangarkar, V. G. Fermentation of Glucose to Lactic Acid Coupled with Reactive Extraction: A Review. *Ind. Eng. Chem. Res.* **2004**, *43* (19), 5969–5982. https://doi.org/10.1021/ie049963n.

(12) Shreve, R. N.; Brink Jr, J. A. *Chemical Process Industries.*; 1977.

(13) Eyal, A. M.; Bressler, E. Industrial Separation of Carboxylic and Amino Acids by Liquid Membranes: Applicability, Process Considerations, and Potential Advantage. *Biotechnol. Bioeng.* **1993**, *41* (3), 287–295. https://doi.org/10.1002/bit.260410302.

(14) Komesu, A.; Maciel, M. R. W.; Filho, R. M. Separation and Purification Technologies for Lactic Acid - A Brief Review. *BioResources* **2017**, *12* (3), 6885–6901. https://doi.org/10.15376/biores.12.3.6885-6901.

(15) Lee, H. D.; Lee, M. Y.; Hwang, Y. S.; Cho, Y. H.; Kim, H. W.; Park, H. B. Separation and Purification of Lactic Acid from Fermentation Broth Using Membrane-Integrated Separation Processes. *Ind. Eng. Chem. Res.* **2017**, *56* (29), 8301–8310. https://doi.org/10.1021/acs.iecr.7b02011.

(16) Emel'yanenko, V. N.; Verevkin, S. P.; Schick, C.; Stepurko, E. N.; Roganov, G. N.; Georgieva, M. K. The Thermodynamic Properties of S-Lactic Acid. *Russ. J. Phys. Chem. A* **2010**, *84* (9), 1491–1497. https://doi.org/10.1134/S0036024410090074.

(17) Talebi, S.; Suarez, F.; Chen, G. Q.; Chen, X.; Bathurst, K.; Kentish, S. E. Pilot Study on the Removal of Lactic Acid and Minerals from Acid Whey Using Membrane Technology. *ACS Sustain. Chem. Eng.* **2020**, *8* (7), 2742–2752. https://doi.org/10.1021/acssuschemeng.9b06561.

(18) Chandrapala, J.; Chen, G. Q.; Kezia, K.; Bowman, E. G.; Vasiljevic, T.; Kentish, S. E. Removal of Lactate from Acid Whey Using Nanofiltration. *J. Food Eng.* **2016**, *177*, 59–64. https://doi.org/10.1016/j.jfoodeng.2015.12.019.

(19) Matsumoto, M.; Hasegawa, W.; Kondo, K.; Shimamura, T.; Tsuji, M. Application of Supported Ionic Liquid Membranes Using a Flat Sheet and Hollow Fibers to Lactic Acid Recovery. *Desalin. Water Treat.* **2010**, *14* (1–3), 37–46.

https://doi.org/10.5004/dwt.2010.1009.

(20) Takegami, S.; Yamada, H.; Tsujii, S. Pervaporation of Ethanol/Water Mixtures Using Novel Hydrophobic Membranes Containing Polydimethylsiloxane. *J. Memb. Sci.* **1992**, *75* (1–2), 93–105. https://doi.org/10.1016/0376-7388(92)80009-9.

(21) Ozcam, A. E.; Petzetakis, N.; Silverman, S.; Jha, A. K.; Balsara, N. P. Relationship between Segregation Strength and Permeability of Ethanol/Water Mixtures through Block Copolymer Membranes. *Macromolecules* **2013**, *46* (24), 9652–9658. https://doi.org/10.1021/ma401957s.

(22) Petzetakis, N.; Doherty, C. M.; Thornton, A. W.; Chen, X. C.; Cotanda, P.; Hill, A. J.; Balsara, N. P. Membranes with Artificial Free-Volume for Biofuel Production. *Nat. Commun.* **2015**, *6* (May), 1–8. https://doi.org/10.1038/ncomms8529.

(23) Mahanthappa, M. K.; Bates, F. S.; Hillmyer, M. A. Synthesis of ABA Triblock Copolymers by a Tandem ROMP-RAFT Strategy. *Macromolecules* **2005**, *38* (19), 7890–7894. https://doi.org/10.1021/ma051535l.

(24) Yu, X.; Jiang, X.; Seidler, M. E.; Shah, N. J.; Gao, K. W.; Chakraborty, S.; Villaluenga, I.; Balsara, N. P. Nanostructured Ionic Separator Formed by Block Copolymer Self-Assembly: A Gateway for Alleviating Concentration Polarization in Batteries. *Macromolecules* **2022**, *55* (7), 2787–2796. https://doi.org/10.1021/acs.macromol.2c00193.

(25) Ilavsky, J. Nika: Software for Two-Dimensional Data Reduction. *J. Appl. Crystallogr.* **2012**, *45* (2), 324–328.

(26) Mazumder, A.; Dobyns, B. M.; Howard, M. P.; Beckingham, B. S. Theoretical and Experimental Considerations for Investigating Multicomponent Diffusion in Hydrated, Dense Polymer Membranes. *Membranes (Basel).* **2022**, *12* (10). https://doi.org/10.3390/membranes12100942.

(27) Kim, J. M.; Dobyns, B. M.; Zhao, R.; Beckingham, B. S. Multicomponent Transport of Methanol and Acetate in a Series of Crosslinked PEGDA-AMPS Cation Exchange Membranes. *J. Memb. Sci.* **2020**, *614* (July). https://doi.org/10.1016/j.memsci.2020.118486.

(28) Yasuda, H.; Ikenberry, L. D.; Lamaze, C. E. Permeability of Solutes through Hydrated Polymer Membranes. Part II. Permeability of Water Soluble Organic Solutes. *Die Makromol. Chemie* **1969**, *125* (1), 108–118. https://doi.org/10.1002/macp.1969.021250111.

(29) Heiranian, M.; Fan, H.; Wang, L.; Lu, X.; Elimelech, M. Mechanisms and Models for

Water Transport in Reverse Osmosis Membranes: History, Critical Assessment, and Recent Developments. *Chem. Soc. Rev.* **2023**, *52* (24), 8455–8480. https://doi.org/10.1039/d3cs00395g.

(30) Wijmans, J. G. H.; Baker, R. W. *The Solution-Diffusion Model: A Unified Approach to Membrane Permeation*; 2006. https://doi.org/10.1002/047002903X.ch5.

(31) Lacuve, M.; Colin, X.; Perrin, L.; Flandin, L.; Notingher, P.; Tourcher, C.; Ben Hassine, M.; Tanzeghti, H. Investigation and Modelling of the Water Transport Properties in Unfilled EPDM Elastomers. *Polym. Degrad. Stab.* **2019**, *168*, 108949. https://doi.org/10.1016/j.polymdegradstab.2019.108949.

(32) Das, G.; Choi, J. H.; Nguyen, P. K. T.; Kim, D. J.; Yoon, Y. S. Anion Exchange Membranes for Fuel Cell Application: A Review. *Polymers (Basel).* **2022**, *14* (6). https://doi.org/10.3390/polym14061197.